LA-UR- 06- 0918

Approved for public release; distribution is unlimited.

Title: DEVELOPMENT OF SIGNAL PROCESSING TOOLS AND HARDWARE FOR PIEZOELECTRIC SENSOR DIAGNOSTIC PROCESSES

Author(s): Timothy G. Overly, LANL, INST-OFF
GyuHae (NMI) Park, LANL, INST-OFF
Charles R. Farrar, LANL, INST-OFF

Submitted to: SPIE INTERNATIONAL SYMPOSIUM ON SMART STRUCTURES AND NONDESTRUCTIVE EVALUATION,SAN DIEGO, CA, MAR. 18-22, 2007.

Los Alamos
NATIONAL LABORATORY

Development of Signal Processing Tools and Hardware for Piezoelectric Sensor Diagnostic Processes

Timothy G. S. Overly, Gyuhae Park and Charles R. Farrar

Engineering Institute, Los Alamos National Laboratory, Los Alamos, USA

ABSTRACT

This paper presents a piezoelectric sensor diagnostic and validation procedure that performs in-situ monitoring of the operational status of piezoelectric (PZT) sensor/actuator arrays used in structural health monitoring (SHM) applications. The validation of the proper function of a sensor/actuator array during operation, is a critical component to a complete and robust SHM system, especially with the large number of active sensors typically involved. The method of this technique used to obtain the health of the PZT transducers is to track their capacitive value, this value manifests in the imaginary part of measured electrical admittance. Degradation of the mechanical/electrical properties of a PZT sensor/actuator as well as bonding defects between a PZT patch and a host structure can be identified with the proposed procedure. However, it was found that temperature variations and changes in sensor boundary conditions manifest themselves in similar ways in the measured electrical admittances. Therefore, we examined the effects of temperature variation and sensor boundary conditions on the sensor diagnostic process. The objective of this study is to quantify and classify several key characteristics of temperature change and to develop efficient signal processing techniques to account for those variations in the sensor diagnosis process. In addition, we developed hardware capable of making the necessary measurements to perform the sensor diagnostics and to make impedance-based SHM measurements. The paper concludes with experimental results to demonstrate the effectiveness of the proposed technique.

Keywords: Sensor Diagnosis, Sensor Validation, Structural Health Monitoring, Impedance Method

1. INTRODUCTION

The primary goal of this paper is to present sensor diagnostic and validation procedures for piezoelectric patches used in structural health monitoring. A robust diagnostic procedure that determines the health of piezoelectric sensor is desired because of the potentially large number of sensors being used in a typical SHM application. In addition, piezoelectric (PZT) sensors are generally weaker than the structure that they monitor, making them the most susceptible part of the system to fail. The procedure that will be outlined here uses the capacitive measurement of the PZT transducer that has been bonded to the structure.

The proposed technique will allow for the monitoring of both the sensor bonding condition and the sensor health itself. Debonding and breakage manifest themselves differently in the capacitive signal, and a classification of those changes was performed. In addition to the basic feature classification of various sensor failure modes, the effect of temperature is also examined. This data allows for the correction of the sensor diagnostic process to environmental variance. Hardware that was developed to make impedance based SHM measurements, is also briefly reviewed in this paper. This hardware was specifically designed to be able to implement the proposed sensor diagnostic algorithm in addition to impedance SHM. Finally, we conclude with experimental results of the demonstrated technique.

1.1. Impedance Method

The sensor diagnostic process that is proposed is based on electromechanical impedance measurements. Liang et al.[1] was the first to develop the theory for impedance based measurements for use in SHM. The theory has been substantially developed by Park et al.[2–4] , Bhalla et al.,[5,6] Giurgiutiu et al.[7–9] and Sun et al..[10]

The basic concept of the impedance method is to use high frequency vibrations to monitor the local area of a structure for changes in structural impedance that would indicate damage or structural change. The monitoring is made possible by using piezoelectric (PZT) sensor/actuators whose electrical impedance is directly related to the structure's mechanical impedance. The impedance measurements can easily give information on changing

parameters, such as resonant frequencies or damping, which allows for the detection and location of damage. The expression for one dimensional electromechanical admittance($Y(\omega)$) of a PZT that is bonded to a structure, which was developed by Liang et al., is given in Equation 1.

$$Y(\omega) = \omega i \frac{wl}{h}\left(\bar{\varepsilon}_{33}^{T}(1-i\delta) - d_{31}^{2}\bar{Y}^{E} + \frac{Z_a(\omega)}{Z_s(\omega)+Z_a(\omega)} d_{31}^{2}\bar{Y}^{E}\left(\frac{\tan\kappa l}{\kappa l}\right)\right) \tag{1}$$

Where w, l, and h are width, length and height of the PZT patch respectively. $Z_s(\omega)$ and $Z_a(\omega)$ are the mechanical impedances of the host structure and of the PZT transducer respectively, κ is the wave number, $\bar{Y}^E$ is the complex Young's modulus, and $\bar{\varepsilon}_{33}^{T}$ is the complex electric permittivity of the PZT transducer along the z axis. In addition $Z_a(\omega)$ is also defined by Equation 2.

$$Z_a(\omega) = \frac{\kappa w h \bar{Y}^E}{i\omega \tan\kappa l} \tag{2}$$

And finally for the one dimensional case, the wave number is defined in Equation 3.

$$\kappa = \omega\sqrt{\frac{\rho}{\bar{Y}^E}} \tag{3}$$

The previous formulas were further developed by Bhalla and Soh,[6] who solved the two dimensional governing equation for $Y(\omega)$, which is given in Equation 4.

$$Y(\omega) = \omega i \frac{l^2}{h}\left(\bar{\varepsilon}_{33}^{T} - \frac{2d_{31}^{2}\bar{Y}^{E}}{(1-\nu)} + \frac{2d_{31}^{2}\bar{Y}^{E}}{(1-\nu)}\left(\frac{Z_{a,eff}(\omega)}{Z_{s,eff}(\omega)+Z_{a,eff}(\omega)}\right)\bar{T}\right) \tag{4}$$

Where $\bar{T}$ is the complex tangent ratio, which in an ideal situation would be equal to $\frac{\tan\kappa l}{\kappa l}$. Equation 4 introduces the idea of effective impedance, in $Z_{s,eff}(\omega)$ and $Z_{a,eff}(\omega)$. It can be seen how these two terms combine to couple the impedances of the structure and the piezoelectric patch. This coupling allows one to measure the mechanical impedance of the structure through the electrical impedance of the piezoelectric patch.

Once a PZT transducer has been bonded to the structure, the impedance-based SHM system is able to monitor the high frequency region of the structure for local damage. The higher frequency range is more sensitive to local damage, as opposed to lower frequency which is more sensitive to global changes or operational condition changes in the system. It has been shown that the wavelength of the signal, used to detect damage of a given size, needs to be smaller than the characteristic length of the damage.[11] To satisfy this requirement and to be able detect incipient damage, the frequency range of 30-400 kHz is usually used.[4] In addition, the maximum frequency that should be considered should usually be below 500 kHz,[12] above this frequency the sensing region is very small and is sensitive to the piezoelectric patch and its bonding conditions and not of the structure. However, depending on the measurement situation, the maximum frequency used is usually well below this boundary.

There has been extensive research performed in recent years on the application of impedance measurements in the field of structural health monitoring. A good review on the topic is presented by Park et al..[4] An important aspect of the impedance method is that the method requires significantly lower power compared to other active-sensing technologies, such as Lamb wave propagation. In addition to the lower power requirements, impedance measurements also have the potential to perform in-situ active sensor diagnosis, which is discussed in this paper. It has been observed by several people including Park[2] and Bhalla[6] that the imaginary admittance of the impedance measurement is an indication of bonding condition, but a efficient signal processing tool that accounts for environmental changes still needs to be accomplished.

1.2. Sensor Diagnostic Process

Methods for determining the health of piezoelectric patches have been examined in previous research. A couple of them specifically make use of the impedance measurements of the piezoelectric patch, although in different ways. Saint-Pierre et al.[13] uses the shape of the first real impedance resonance and its change to determine the state of the bonding condition. Guirgiutiu and Zagrai[9] propose a similar technique using the attenuation of the first imaginary impedance resonance for damage detection. Pacou et al.[14] discusses the use of the shift of the first natural frequency of the piezoelectric patch before and after bonding as a possible method for determining bonding condition.

There are several disadvantages to the above methods. First, they are not sensitive to small debonding in the PZT. Secondly they all require relatively high frequency measurements to determine the bonded first natural frequency. A standard impedance analyzer can be used to make a measurement into the 600 kHz range and up, which is needed in these methods. Current SHM nodes that are used for the impedance based SHM are not able to make impedance measurements into that range.[15] This frequency requirement makes these techniques generally unsuitable for field deployment using currently available sensor nodes. Finally the absolute number of data points that need to be collected for sensor diagnosis is quite high compared to the method purposed in this paper. The higher number of data points demands more from the SHM node, which generally have very limited storage capacity and RAM.

Bhalla and Soh,[6] in addition to the formulations in Section 1.1 suggest that the imaginary part of the admittance measurement is more sensitive to bonding conditions, and therefore could be useful in determining the bond health. This relationship was further developed by Park et al.,[2,16] who showed the initial relationship between bonding condition and the slope of the imaginary admittance measurement (susceptance). This technique is based on the admittance measurement of a free PZT that is shown in Equation 5 and the equation for the bonding layer's effect on the electrical admittance, which is given in Equation 6.

The equation for a PZT in a free state that was developed in Park et al.[2] is given in Equation 5.

$$Y_{free}(\omega) = i\omega \frac{wl}{t_c}(\bar{\varepsilon}_{33}^{T}(1 - i\delta)) \tag{5}$$

The equation for the bonding layer effects is achieved by allowing the structural impedance in Equation 1 to approach infinity.

$$Y_{bond}(\omega) = i\omega \frac{wl}{t_c}(\bar{\varepsilon}_{33}^{T}(1 - i\delta) - d_{31}^{2}\bar{Y}_{p}^{E}) \tag{6}$$

Equations 5 and 6 show that the same PZT will have a different capacitive value from a free-free condition to a surface-bonded condition. The bonding of the sensor would cause a downward shift in the electrical admittance of the free PZT by a factor of $d_{31}^{2}Y_{p}^{E}$. This change in slope would allow for the health of the bonding condition and the physical health of the transducer to be assessed with a measurement of the susceptance.[2]

1.3. SHM Devices

The sensor diagnostic algorithm proposed here is specifically designed to be used in the field with current and near term deployable structural health monitoring nodes. In particular, the wireless impedance device developed by the authors was of primary consideration.[17] The device is pictured in Figure 1, and this figure shows both side of the Wireless Impedance Device or WID.

This device was designed to replace laboratory impedance analyzers for in-field structural health monitoring. A table with important comparison information between the WID and a HP 4294A Impedance Analyzer is shown in Table 1. The WID fulfills much of the needed requirement for SHM, including the necessary frequency range, power requirements at a very low cost. More in-depth information can be found in Overly et al..[17]

Our hardware follows the same design philosophy that was previously developed by Grisso[18] and Grisso et al.,[19] but with different components and capabilities. Their system uses discrete components for impedance measurements, while our device uses an integrated solution. Their system can also be considered as potential

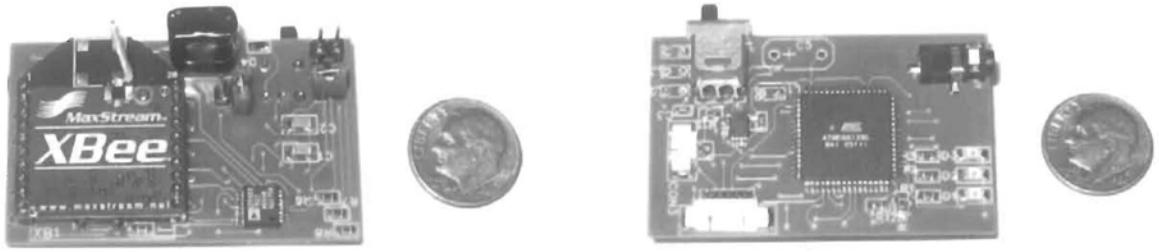

(a) Top (b) Bottom

Figure 1. Both sides of the Wireless Impedance Device

hardware for the sensor diagnostic algorithm and is currently being investigated by the researchers at Virginia Tech.

2. EFFECTS OF SENSOR FAILURE

Various types of sensor failure will affect imaginary admittance in different ways. The first step in the diagnostic process is to quantify those changes for different bonding and sensor conditions. The classification will allow the imaginary admittance measurements to be used in a meaningful way in a sensor diagnostic procedure. The two main types of sensor failure being examined are sensor debonding and sensor breakage.

2.1. Debonding

Sensor debonding is a failure mode of considerable concern. It is of concern, because unlike some of the other failure modes it is not readily noticeable upon visual inspection. Debonding may occur in a situation where the structure may not have sustained any damage, i.e. a strain large for the PZT but within the operating parameters of the structure or the long-term degradation of the adhesive bond.

To test the effects of debonding, sixteen 12.7mm PZT patches were bonded to a 6.35mm thick aluminum plate. Nine were bonded with epoxy and nine with super glue. In each set of nine, three were bonded fully, three were bonded with 25 percent debonding and the remaining three were bonded at 50 percent. Two adhesives were used to test if different adhesives contribute differently to the change in susceptance. This simulation of debonding was achieved by using release paper to restrict the bonding percentages of the sensor. Specifically, the PZT was bonded a corresponding percent of the total area on top of double layer of release paper. Photos of the bonded sensors are shown in Figure 2.

The debonding of the sensors has an effect on the sensor diagnostic indicator that we are examining, the slope of the susceptance. The slope changes in a repeatable and consistent manner with debonding percentages. Figure 3 shows two graphs, both at room temperature, of the effect of debonding percentages on the susceptance. Figure 3(a) and 3(b) are of super glue and epoxy bonded patches respectively. The slope of the susceptance decreases with debonding. It can be seen in each graph that there is a progression of the measurements from the highest slope, a reference free-free set, to the lowest slope, the fully bonded case. This decrease is consistent with

	4295A	WID
Frequency Range	40 Hz - 110mHz	5kHz -100kHz
Sweep Points	801	512
Power Supply	120V	2.8V
Cost	$41,000	$200

Table 1. Comparison of key features between the Agilent 4294A and the WID

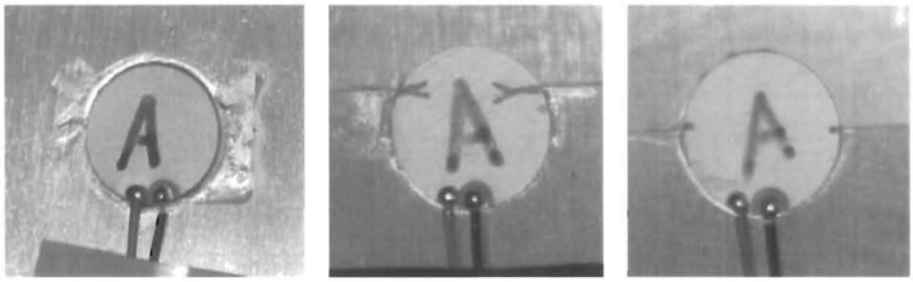

(a) 0% Debonding (b) 25% Debonding (c) 50% Debonding

Figure 2. Various debonding percentages on 5.5*mm* PZT patches

a previous study,[2] but it shows that the percent of change not only indicates debonding, but also the amount of debonding.

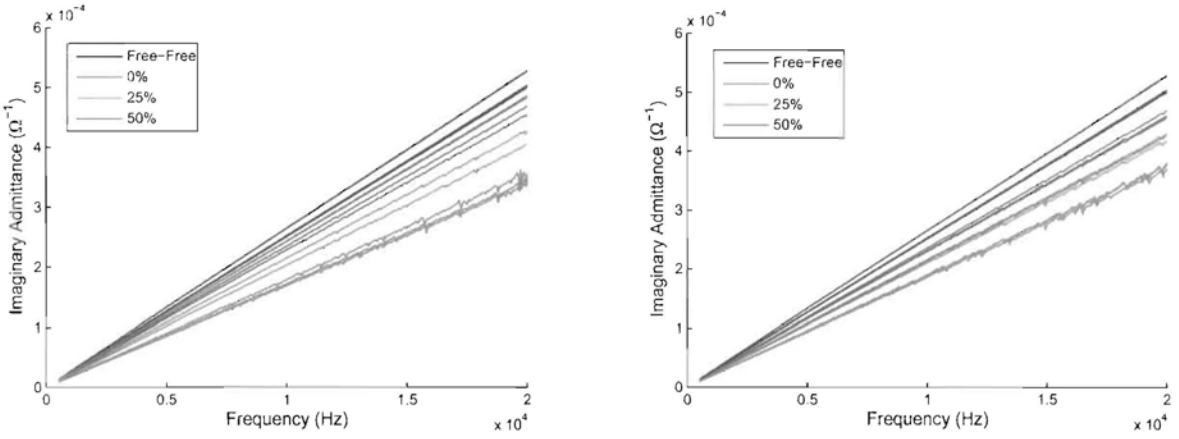

(a) Super Glue (b) Epoxy

Figure 3. The slope of the susceptance increases with debonding percentage

2.2. Breakage

The second sensor failure mode to be investigated is sensor breakage. After a potentially damaging event on structure, it is possible that the PZT patch that is being used to monitor the structure may have been damaged, causing a potentially erroneous measurement of the structure. To investigate the effects of such an occurrence, six 12.7mm PZT patches that were bonded to a 6.35mm thick aluminum plate, were broken and cut at specific percentages of their total area, and then impedance measurements were taken. Three patches were broken or cut to reduce the total area by 25 percent, and three patches were broken or cut at to reduce the total area by 50 percent. Two of each three were broken with a chisel, to more accurately simulate a damage event. The remaining patches were cut with an abrasive wheel to insure a more accurate reference case. Figure 4(a) shows the 25 percent breakage case, and Figure 4(b) shows the 50 percent breakage case.

Impedance measurement of these patches was taken prior to breakage and post breakage, allowing for a comparison of the actual change of capacitive value for each sensor. Imaginary admittance measurements were taken of free-free baseline cases, and all the measurements are shown in Figure 5. It can be seen in Figure 5 that the slope of the imaginary admittance is proportional to the breakage percentage. As the percent increases, the slope decreases. There is some variance in the slopes of each group, which can most likely be attributed

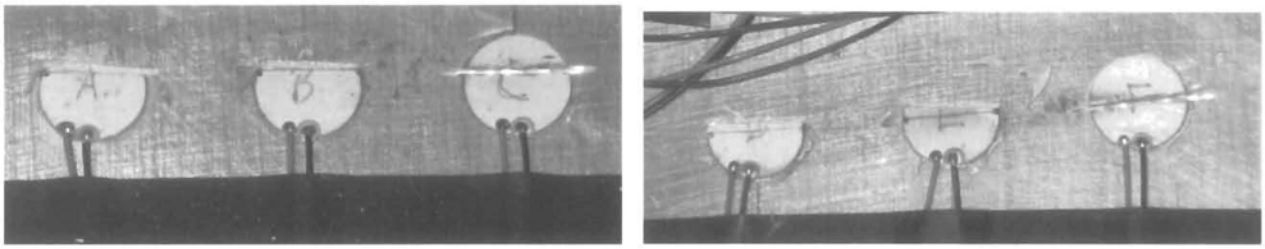

(a) 25 Percent (b) 50 Percent

Figure 4. The PZT patches were broken using both a chisel and an abrasive cutting wheel

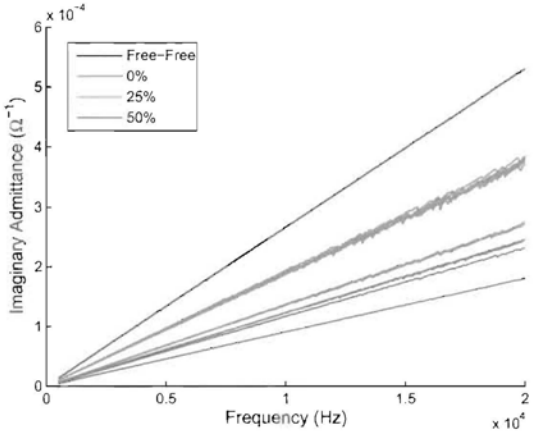

Figure 5. The slope of the imaginary admittance decreases as breakage area increases

to the inconsistent nature of the fractures. Figure 4 shows that the post breakage patch fragments are not a consistent size, they are approximately a 25 and 50 percent reduction, but do have some variance. The line with the greatest decrease in slope corresponds to the cut 50 percent patch, which has the smallest final area, demonstrating a further correlation between final patch size and slope.

3. EFFECTS OF TEMPERATURE CHANGES

As temperature changes the physical properties of the structure, the bonding layer and PZT sensor will also change. The result is a shift in the imaginary admittance measurements made in the previous section. The extent of these effects is what is examined in this section. In order to make the sensor diagnosis procedure viable in a real world setting, temperature effects on the susceptance were examined. Both broken and debonded patches were examined for the effect that temperature had on the susceptance for each failure mode.

3.1. Debonding

The test setup was the same 6.35mm aluminum plate with the debonded patches that was used in Section 2.1. In addition, the plate was heated and impedance measurements were taken at incremental temperatures. The plate was heated from room temperature to $135°F$, and the impedance measurements were taken from 500 to 20,000 Hz using an Agilent 4294A impedance analyzer. Once the imaginary admittance measurement was taken at each temperature, a linear least-squares fit was performed on the measurement to obtain the slope of the signal. This slope value is what was compared from one temperature to the next. The linearity of the signal should be checked before this fit is performed because some structures may have resonances within the frequency range causing an error in the slope value.

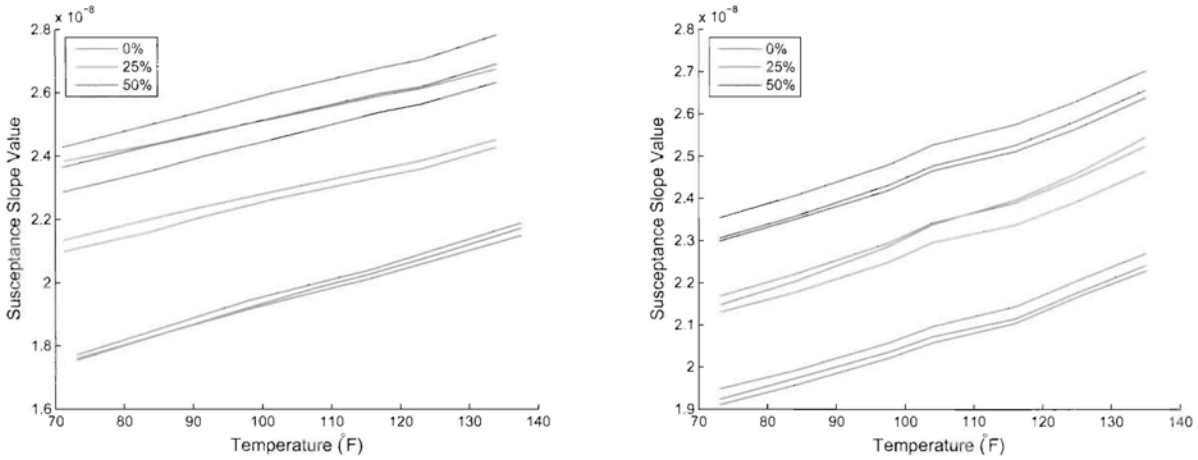

(a) Super Glue (b) Epoxy

Figure 6. The slope change of susceptance verse temperature for three different bonding percentages for both a) super glue and b) epoxy

The primary concern was that the slope of the susceptance would vary differently among different bonding and sensor conditions, making it more difficult to assess the bonding condition though the examination of the admittance slope. The results of the temperature test on debonded patches are shown in Figure 6. It can be seen in this graph that as temperature increases the capacitance value of the PZT increases. It can also be seen that the patches bonded with epoxy and superglue have a similar slope change with temperature. From room temperature to a temperature of $135°F$ all the conditions that were bonded with epoxy and super glue $0.35e^{-8}$ increase in the slope. Because of the parallel nature of the slope decrease, a sensor diagnostic algorithm that is invariant of temperature changes can be developed. If the algorithm uses a system to find outlying PZT sensors, the procedure can be temperature independent, because an outlier will remain outlier at any temperature.

3.2. Breakage

As an additional check, the effects of temperature on the susceptance measurements of broken patches were also examined. The procedure was the same as the debonding temperature test, but using the broken patches from Section 2.2. The result of broken sensor temperature test is shown in Figure 7.

As with the debonded sensors, the broken sensors behave in a predictable manner, with all of the breakage cases performing in a parallel manner. The fact that all the patches stay in distinct regions also makes sensor breakage detectable through outlier detection.

4. SIGNAL PROCESSING FOR DIAGNOSTICS OF SENSOR ARRAYS

In this method, we propose a procedure that uses the measured susceptance values of PZT transducers to allow for the state of the transducers to be obtained without the need for pre-stored baseline measurements. When a group of sensors is bonded to a similar structure, there is the opportunity to compare one sensor to another. This comparison can occur because the sensors are all exposed to the same environmental conditions and so those effects can be removed. Through a process of outlier detection, sensors with errant bonding or health conditions are identified.

For an array of sensors, the task lies in determining which of the sensors is not part of the healthy group. The algorithm takes advantage of the characteristic that the removal of an unhealthy patch will cause a greater decrease in the standard deviation of the group of sensors, than will the removal of a health sensor. A process was developed to test the effect each sensor had on the overall standard deviation of the group of signals, and to determine at what point the change occurred from unhealthy to healthy sensors. This process is documented here:

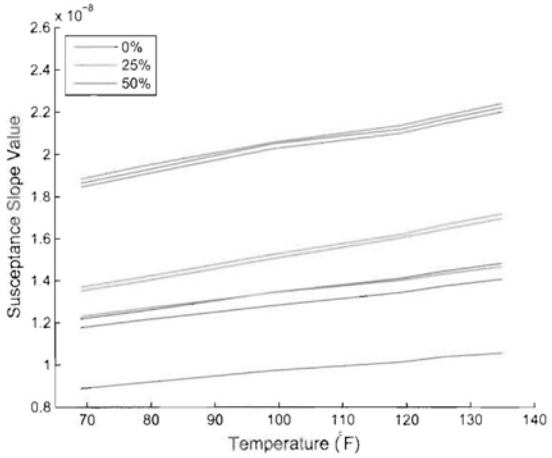

Figure 7. The slope change of susceptance verse temperature for various breakage percentages bonded with super glue

1. The slope of each of the PZT transducer's susceptance signals, which is a measure of the capacitive value, is calculated in a least-squares manner.
2. The transducer in the group that contributes, by its removal, to the maximum reduction in the standard deviation is found.
   (a) One of the PZT transducer's susceptance signals is removed and the remaining group's standard deviation is recalculated.
   (b) The PZT transducer with the maximum influence on the standard deviation is recorded and removed from future iterations.
   (c) Steps 2a and 2b are repeated until two sensors remain.
3. The sensors are arranged from the one that has the most influence to the final two sensors. The sensor that corresponds to the maximum distance from the total change is determined, and is recorded as the sensor that starts the healthy patches. The sensors with a greater influence than this patch are determined to be unhealthy.

A visual representation of the above procedure is shown in Figure 8. The maximum number of recommend unhealthy patches is limited to less than half of the total number of sensors. If a sensor's effect on the standard deviation is negative (it falls above the overall slope change), no sensors are recommended for replacement, because the total slope change does a reasonable job at approximating the individual slope change. The frequency range that is used in determining the slope of the susceptance should be examined to make sure there is no major structural resonance that would induce error into the least squares fit of the line.

A MATLAB script was written to implement the above procedure. As an initial test two plate structures that had 12.7mm PZT sensors bonded to them were examined. The first plate was a 1.6mm thick aluminum plate that measured 122cm x 122cm. This plate is shown in Figure 9(a), and has very uniform properties. Other structures may have a slightly higher variance due to structure irregularities. To investigate this possibility a second plate was examined that was 13mm thick and had aluminum honeycomb structure. The second plate measured 61cm x 61cm and it is shown in Figure 9(b). Each of the plates had sensors initially bonded to them, with varying degrees of health.

The sensor diagnostic algorithm was run on each plate. The output of the proposed algorithm is a hybrid plot with the upper plot showing all of the susceptance measurements with color coding corresponding to the lower plot. The lower plot shows the effect of the reducing the sample number, with the x-axis showing which sensor

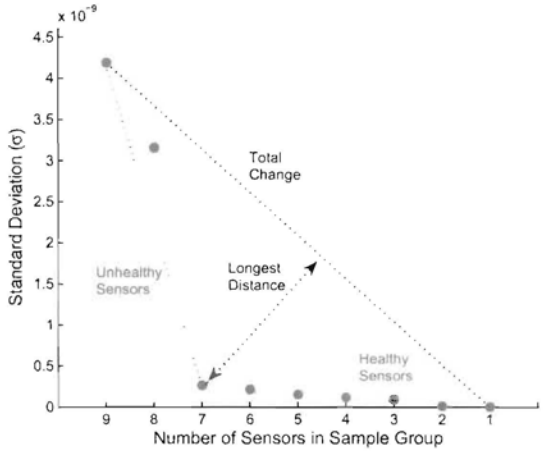

Figure 8. The longest distance from the overall change corresponds to the change from unhealthy to healthy patches

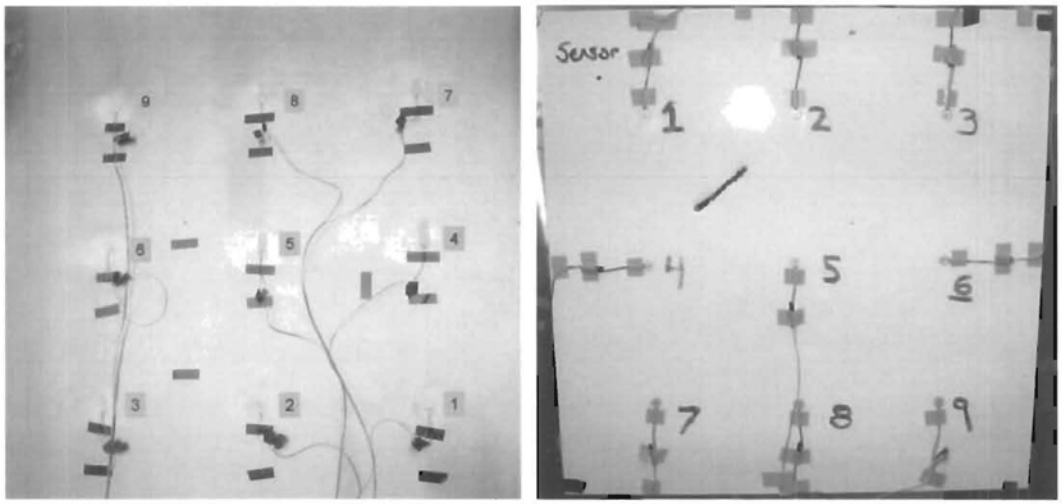

(a) 1/16" Aluminum (b) Aluminum Honeycomb

Figure 9. Two plates with poorly bonded patches were used to test the sensor array diagnostic algorithm

numbers are recommended for removal. The lower plot also has a line delineating the healthy patches from the unhealthy ones. The results from Plate 1 are shown in Figures 10(a) and 10(b) and the results from Plate 2 are shown in Figures 10(c) and 10(d). When the algorithm was run on each plate, several sensors on the solid aluminum plate were recommended for replacement and one sensor on the honeycomb plate was recommended for replacement. Those sensors were replaced and the algorithm was run again on each plate. Both plates passed the algorithm the second time. It should be noted that the honeycomb plate does have a grouping of values due to the heterogeneous nature of the material.

The main advantage of looking for the change in the data in this manner, is that no absolute value for the effect of a sensor is required. The lack of a required pre-stored baseline allows this system to be used on a variety of structures with no training set required. A further test of the procedure was performed by bonding a sensor on each of the plates at a 50 percent bond area. The sensors were bonded on each plate at the number seven location, and were bonded in the same manner as is shown in Figure 2(c). Admittance measurements were taken

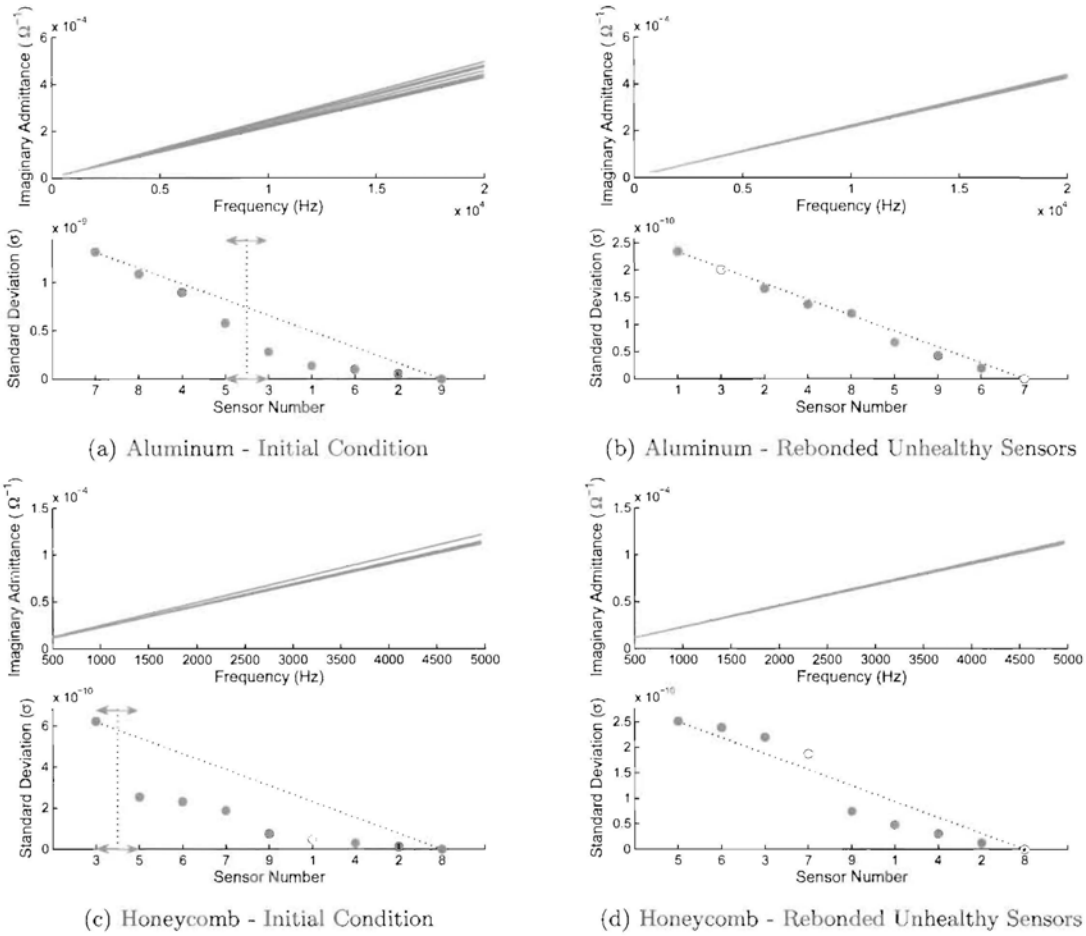

(a) Aluminum - Initial Condition

(b) Aluminum - Rebonded Unhealthy Sensors

(c) Honeycomb - Initial Condition

(d) Honeycomb - Rebonded Unhealthy Sensors

Figure 10. Each plate passes the sensor test after the recommended unhealthy sensors are removed and new sensors are bonded in their place

with all the healthy sensors from Figures 10(b) and 10(d) except the debonded PZT sensor located at position number seven. The resulting measurements are shown in Figure 11. From the two plots the algorithm correctly identifies the poorly bonded PZT on the solid aluminum plate and the honeycomb plate.

In order to compensate for temperature and environmental effects we propose that multiple sensors should be used in a given SHM system whenever possible. These extra sensors provide redundancy for measurements and allow for an efficient and reliable method for sensor diagnostics. The imaginary admittance slope comparison will work with a group of sensors. Even during temperature changes, all the sensors will shift the same percentage for any given temperature change, as seen in Section 3. Care does have to be taken to make sure that the sensors being analyzed are exposed to the same environmental conditions, or false positives may occur.

5. CONCLUSIONS

The imaginary impedance measurement shows a great deal of promise for use in the structural health monitoring field as sensor diagnostic measurements. The method can be readily used with sensor arrays with no pre-stored baseline measurements. The method can also distinguish between sensor breakage and sensor debonding and give relative percentages of each type of sensor failure. In addition, impedance based measurement in the lower frequency ranges proposed here are more easily implemented with currently available hardware, and have lower

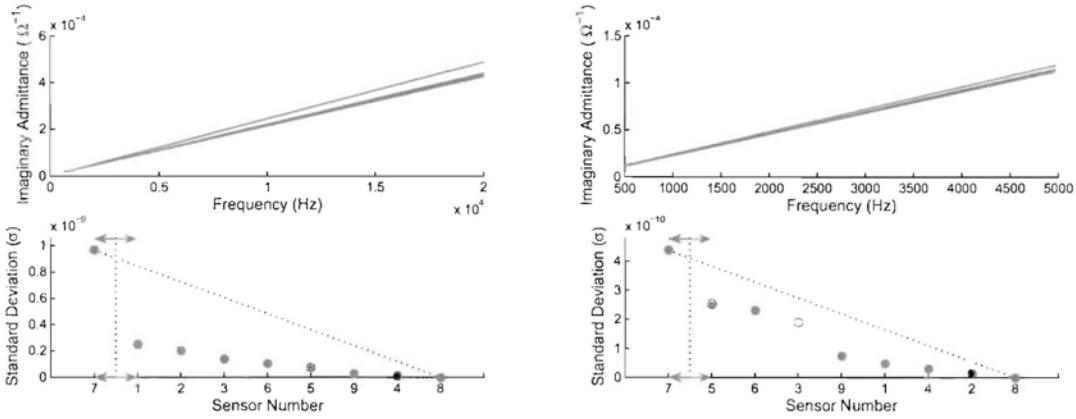

(a) 1/16" Aluminum

(b) Aluminum Honeycomb

Figure 11. The algorithm correctly identifies the debonded sensor on the solid plate and over estimates the number of damaged sensors on the honeycomb plate.

power requirements than other methods. Future work on the method should include the development of the single sensor procedure to include a robust regression technique, or the search for a temperature independent feature of the impedance measurement.

REFERENCES

1. C. Liang, F. P. Sun, and C. A. Rodgers, "Coupled electromechanical analysis of adaptive material systems - determination of the actuator power consumption and system energy transfer," *Journal of Intelligent Material Systems and Structures* **5**, pp. 12–20, 1994.
2. G. Park, C. R. Farrar, A. C. Rutherford, and A. N. Robertson, "Piezoelectric active sensor self-diagnostics using electrical admittance measurements," *ASME Journal of Vibration and Acoustics* **128**, pp. 469–476, August 2006.
3. G. Park, T. G. Overly, M. J. Nothnagel, C. R. Farrar, D. M. Mascareas, and M. D. Todd, "A wireless active-sensor node for impedance-based structural health monitoring," in *Proceedings of US-Korea Smart Structures Technology for Steel Structures,*, November 2006.
4. G. Park, H. Sohn, C. R. Farrar, and D. J. Inman, "Overview of piezoelectric impedance-based health monitoring and path forward," *The Shock and Vibration Digest* **35**, pp. 451–463, 2003.
5. S. Bhalla, A. S. K. Naidu, C. W. Ong, and C.-K. Soh, "Practical issues in the implementation of electro-mechanical impedance technique for nde," in *Proceedings of SPIE*, E. C. Harvey, D. Abbott, and V. K. Varadan, eds., **4935**, pp. 484–494, November 2002.
6. S. Bhalla and C. K. Soh, "Electromechanical impedance modeling for adhesively bonded piezo-transducers," *Journal of Intelligent Material Systems and Structures* **15**, pp. 955–972, December 2004.
7. V. Giurgiutiu and A. Zagrai, "Damage detection in thin plates and aerospace structures with the electro-mechanical impedance method," *Structural Health Monitoring* **4**, pp. 99–118, 2005.
8. V. Giurgiutiu, A. Zagrai, and J. J. Bao, "Damage identification in aging aircraft structures with piezo-electric wafer active sensors," *Journal of Intelligent Material Systems and Structures* **15**, pp. 673–687, September/October 2004.
9. V. Giurgiutiu and A. N. Zagrai, "Embedded self-sensing piezoelectric active sensors for on-line structural identification," *Transactions of the ASME* **124**, pp. 116–125, January 2002.
10. F. P. Sun, Z. Chaudhry, C. Liang, and C. A. Rogers, "Truss structure integrity identification using pzt sensor-actuator," *Journal of Intelligent Material Systems and Structures* **6**, pp. 134–139, January 1995.

11. J. P. Stokes and G. L. Cloud, "The application of interferometric techniques to the nondestructive inspection of fiber-reinforced materials," *Experimental Mechanics* **33**, pp. 314–319, 1993.
12. J. Esteban, *Modeling of the Sensing Region of a Piezoelectric Actuator/Sensor*. PhD thesis, Virginia Polytechnic Institute and State University, Blacksburg, VA, 1996.
13. N. Saint-Pierre, Y. Jayet, I. Perrissin-Fabert, and J. C. Baboux, "The influence of bonding defects on the electric impedance of a piezoelectric embedded element," *Journal of Physics D: Applied Physics* **29**, pp. 2976–2982, December 1996.
14. D. Pacou, M. Pernice, M. Dupont, and D. Osmont, "Study of the interaction between bonded piezo-electric devices and plates," in *1st European Workshop on Structural Health Monitoring*, (155), 2002.
15. J. P. Lynch and K. J. Loh, "A summary review of wireless sensors and sensor networks for structural health monitoring," *The Shock and Vibration Digest* **38**, pp. 91–128, March 2006.
16. G. Park, C. R. Farrar, F. L. di Scalea, and S. Corria, "Performance assessment and validation of piezoelectric active-sensors in structural health monitoring," *Smart Materials and Structures* **15**, pp. 1673–1683, December 2006.
17. T. G. Overly, G. Park, C. R. Farrar, and R. J. Allemang, "Compact hardware development for shm and sensor diagnostics using admittance measurements," in *Proceedings of the IMAC-XXIV*, SEM, February 2007.
18. B. L. Grisso, "Considerations of the impedance method, wave propagation, and wireless systems for structural health monitoring," Master's thesis, Virginia Polytechnic Institute and State University, 2004.
19. B. L. Grsso, L. A. Martin, and D. J. Inman, "A wireless active sensing system for impedance-based structural health monitoring," in *Proceedings of the IMAC-XXIII*, 2005.